



Effect of double doping, Li and Se, on the high-temperature thermoelectric properties of Cu_2Te

Md. Mofasser Mallick¹ · Satish Vitta²

Received: 9 December 2019 / Accepted: 20 January 2020 / Published online: 30 January 2020
© Springer Science+Business Media, LLC, part of Springer Nature 2020

Abstract

Cuprous chalcogenide, Cu_2Se , attracted attention due to its large Seebeck coefficient coupled with low thermal conductivity, facilitated by the presence of disordered Cu-ions in the structure of Cu–Se. This compound is thermally unstable prompting investigation of its analogue Cu_2Te which has a lower figure-of-merit zT due to its high charge carrier concentration. In the present work, a dual substitution, both cation and anion by Li and Se, respectively, has been attempted to enhance zT . The $\text{Cu}_{2-x}\text{Li}_x\text{Te}_{1-y}\text{Se}_y$ alloys have been synthesized by a simple, conventional arc melting process and investigated without subjecting to any further processing. The room temperature microstructure shows a plate-like layered nanostructure in the grains with the grains oriented in random directions. The alloys at room temperature have two polymorphic phases, superstructured hexagonal and orthorhombic, co-existing in all the alloys. The alloys exhibit a degenerate semiconducting behavior in the range 300–1000 K with the conductivity decreasing from $\sim 3000 \text{ Scm}^{-1}$ to 700 Scm^{-1} . All the alloys show a hole dominant Seebeck coefficient which increases with temperature from ~ 30 to $135 \mu\text{VK}^{-1}$. The alloy with dual substitution, Li-0.1 and Se-0.03, has the highest power factor of $1.6 \text{ mWm}^{-1} \text{ K}^{-2}$ at 1000 K. Its low thermal conductivity in the complete range $< 1.5 \text{ Wm}^{-1} \text{ K}^{-1}$ results in increasing the zT to 1.0 at 1000 K, an increase of 130% compared to the undoped alloy. These alloys are found to be thermally and temporally stable with no significant power loss either due to thermal cycling or aging.

1 Introduction

Chalcogen alloys have been an important class of materials for thermoelectric energy conversion starting with Bi_2Te_3 and PbTe [1–5]. Among these, the binary cuprous chalcogenide alloys Cu_2X , X=S, Se and Te have recently attracted attention due to the unique thermal transport shown by Cu_2Se [6–10]. This alloy has a layered structure formed by Cu–Se, while the Cu^- ions are distributed randomly between these layers at high temperatures. This disordered arrangement of Cu^- ions leads to very low lattice thermal conductivity and coupled with the high Seebeck coefficient results in high figure-of-merit zT at high temperatures [11]. The negative impact of loosely bound Cu^- ions is its thermal stability and reliability. Also, thermal cycling and aging has been found to result in Se loss which

changes the physical properties and hence zT [12]. The alloy Cu_2Te which belongs to this class of cuprous chalcogenide has been investigated for high-temperature thermoelectric application as it has similar layered structure. The main advantage of this alloy has been its relative thermal stability compared to Cu_2Se [13, 14]. Its thermoelectric performance however is far inferior compared to Cu_2Se due to its inherently large charge carrier concentration which increases both electrical and thermal conductivities and reduces the Seebeck coefficient. This apparently high carrier concentration however is found to be non-intrinsic and depends on the method of synthesis. The SPS processed alloy has a carrier concentration of 10^{21} cm^{-3} which decreased to 10^{20} cm^{-3} for a non-SPS-processed sample [15]. The reduced carrier concentration not only decreased the thermal conductivity but also increased the Seebeck coefficient. At room temperature, Cu_2Te has been found to exist in two different polymorphic forms—hexagonal and orthorhombic and the fraction of these phases has an effect on the thermoelectric properties [13]. These results clearly indicate that transport properties in Cu_2Te are governed by the type of polymorphic phase present and the nature of defects in this phase. An alternative strategy which has been used to enhance the performance of Cu_2Te is partial substitutions as

✉ Satish Vitta
satish.vitta@iitb.ac.in

¹ Light Technology Institute, Karlsruhe Institute of Technology, Kaiserstraße 12, 76131 Karlsruhe, Germany

² Department of Metallurgical Engineering and Materials Science, Indian Institute of Technology Bombay, Mumbai 400 076, India

well as introduction of over-stoichiometric elements which should reduce the effective charge carrier concentrations [16, 17]. Partial substitution of Cu with Sn which has more valence electrons to donate and hence reduce the effective hole concentration leads to reduced electrical conductivity but also reduced thermal conductivity which further leads to an increased figure-of-merit. A similar phenomenon has been observed in Ag-over doped Cu_2Te wherein conductivities were significantly reduced. Substitution of Cu with Ga in Cu_2Te is found to enhance thermoelectric performance increasing Seebeck coefficient and electrical conductivity through simultaneous decrease of carrier concentration and increasing carrier mobility [18]. Recently, thermoelectric figure-of-merit is also reported to be enhanced by > 300% by introducing up to 50 wt% of Ag_2Te in Cu_2Te , which is primarily due to reduction in charge carrier concentration [19]. A zT value of ~ 1 has been achieved in In-substituted Cu_2Te by alloying it with pristine compound [20]. Apart from improving zT value, low cost and facile synthesis processes of synthesizing thermoelectric materials are also important. In general, synthesis processes of single-phase chalcogenides happen to be rigorous and time taking [15]. At first, elements in stoichiometric ratio are melted followed by annealing of the ingot for a long period of time in a vacuum-sealed quartz tube. The ingot then is ground into powder and consolidated into pellets using spark plasma sintering at high pressure. A modified one-step synthesis of chalcogenides using arc melting technique would be much faster and cost effective.

In the present work, a dual substitution strategy has been used together with simple and minimal processing to increase the figure-of-merit. The divalent Cu has been substituted with monovalent Li, while Te has been partially substituted with isoelectronic Se. The monovalent Li is highly electropositive compared to Cu and hence results in an increase in ionic character of bonding between Li and Te. This should lead to a decrease in effective charge carriers and thus decrease electrical and thermal conductivity while enhancing the Seebeck coefficient. This effect is anticipated to be more predominant compared to the simple effect of monovalent substitution in divalent sites which results in increasing the effective charge carrier concentration. Se on the other hand is isoelectronic with Te and hence is not expected to alter the charge transport properties significantly. The thermal conductivity of these doped alloys is expected to decrease due to enhanced alloy scattering of phonons.

2 Experimental methods

The $\text{Cu}_{2-x}\text{Li}_x\text{Te}_{1-y}\text{Se}_y$ ($x=0, y=0$; $x=0.1, y=0$; $x=0.1, y=0.03$) alloys have been synthesized by conventional arc melting in Ar atmosphere using high-purity elements. Before melting, a cylindrical stack of elements was made by cold

pressing the required amount of elements. The higher melting Cu was at the top of the stack, while the lower melting, high vapor pressure elements Te, Se and Li were at the bottom. Since arcing takes place at the top, loss of high vapor pressure elements Te, Se and Li is minimized by adopting this stacking sequence for melting. The resulting ingot was flipped and melted several times in order to homogenize the alloy completely. The structural and physical properties of the as-prepared alloys were investigated without subjecting them to any further elevated temperature, treatment or consolidation. The density in all the cases was found to be nearly 100% with respect to that of the theoretical density of $\sim 7.3 \text{ g cm}^{-3}$. The elevated temperature Seebeck coefficient and electrical resistivity were measured in Helium atmosphere using ZEM-3 M8 system. Temperature-dependent thermal diffusivity and heat capacity were measured using Netzsch LFA-457 and DSC 204 F1 systems, respectively. The microstructural analysis was performed using a combination of X-ray diffraction, scanning electron microscopy, energy dispersive X-ray spectroscopy (EDS) and inductively coupled plasma atomic emission spectroscopy (ICP-AES).

3 Results and discussion

The alloy Cu_2Te exhibits several polymorphic forms and at room temperature some of them have been found to coexist [21]. In order to check the presence of these polymorphs, X-ray diffraction was performed and the results are shown in Fig. 1a. The diffraction pattern could be indexed to the presence of two phases—a hexagonal phase belonging to the space group $P3m1$ and an orthorhombic phase with a superstructure. A comparison of the diffraction patterns from the 3 different alloys with the standard diffraction patterns from hexagonal and orthorhombic polymorphs clearly shows that both forms are present in the alloys in significant fractions. These results clearly show that presence of polymorphic forms as well as their volume fractions depends on processing methodology and the actual chemical composition of the alloys. The lattice parameters of this hexagonal phase are: $a=0.936 \text{ nm}$ and $c=2.163 \text{ nm}$ corresponding to a c/a ratio of 2.59, far higher than the ideal value of 1.63. This is due to the presence of loosely bound Cu-ions in between the Cu-Te layers which tend to extend the lattice along the c -direction. This hexagonal phase has a superstructure whose unit cell parameters are $a=2a_0$ and $c=3c_0$ where a_0 and c_0 are the unit cell parameters of the Nowotny phase [22, 23]. The orthorhombic phase has the unit cell parameters of $a=0.732 \text{ nm}$, $b=2.224 \text{ nm}$ and $c=3.646 \text{ nm}$. The large value of unit cell parameters clearly shows the effect of defects in these structures such as vacancies and twins. The fractured surface shows clearly the layered plate-like morphology, Fig. 1b, present in each of the grains. These grains

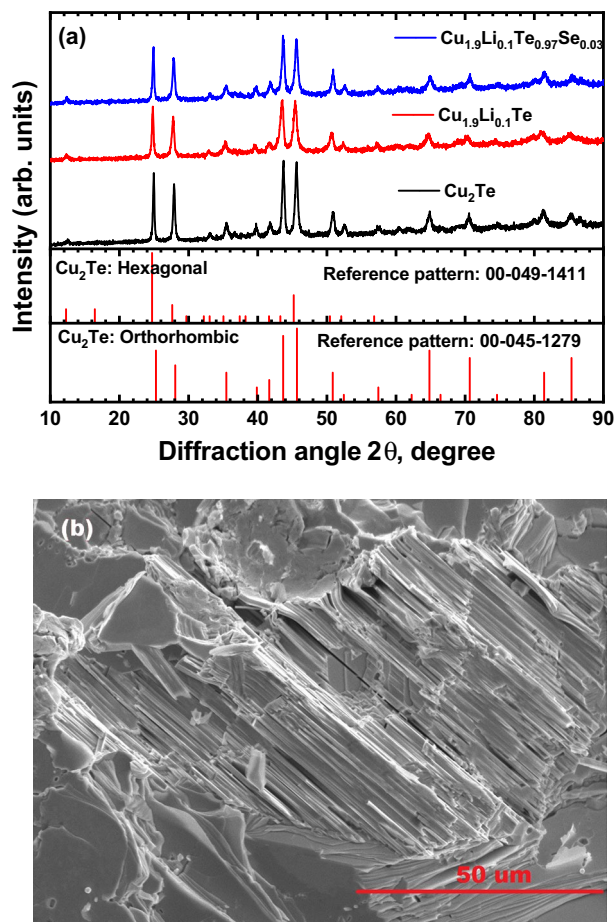


Fig. 1 **a** The X-ray diffraction pattern from the undoped and doped alloys show clearly identical patterns indicating the presence of similar phases in all the alloys. A comparison with standard patterns from hexagonal and orthorhombic polymorphs (shown at the bottom) of Cu_2Te confirms the presence of these two phases in the three alloy. **b** The scanning electron micrograph of the fractured surface shows plate-like morphology of the grains in undoped alloy. The layered morphology is present in all the grains indicating that this is inherent growth behavior of Cu_2Te independent of crystal structure of the polymorphs

with plate-like layered morphology are randomly distributed and indicate typical as-solidified microstructure with no preferred orientation or alignment. An interesting feature is that all the grains have plate-like layered morphology irrespective of their crystal structure. The chemical composition of

the alloys determined by energy dispersive X-ray spectroscopy in the scanning electron microscope is given in Table 1. The chemical composition shows a slight loss of Te, Se and a significant loss of Li due to evaporation during the arc melting process of alloy making. This results in excess Cu being present in all the alloys compared to the stoichiometric composition limit. The presence of excess Cu and the formation of hexagonal and orthorhombic polymorphs is quite unusual. It has been reported that formation of Cu vacancies by phase separation to $\text{Cu}_{2-\delta}\text{Te}$ and Cu_δ leads to stabilization of non-Nowotny structures such as monoclinic or tetragonal and trigonal [23, 24]. At a non-stoichiometry δ of 0.20–0.22, a structural transition has been observed into an hexagonal superstructure stabilized by vacancies. The number density of vacancies has been found to reduce as $\delta \rightarrow 0$ and the alloy becomes near stoichiometric. Hence, the formation of phases with hexagonal superstructure and orthorhombic structure in non-stoichiometric compound such as $\text{Cu}_{2+\delta}\text{Te}$ in the present work clearly indicates that excess Cu is present in the form of interstitials and in between Te layers. The hexagonal and orthorhombic structures can be stabilized either by the presence of Cu vacancies or interstitials.

The high-temperature thermoelectric properties of substituted alloys and the undoped alloy have been investigated as a function of temperature in the range 323–1023 K and compared with the reported values of undoped Cu_2Te . The variation of electrical conductivity with temperature is shown in Fig. 2a together with the results of undoped alloy electrical conductivity reported in Ref. [16]. The undoped alloy synthesized in the present work has lower electrical conductivity at all temperatures compared to earlier reported values. This is because the undoped alloy synthesized in the present work has two polymorphic phases and slightly excess Cu compared to stoichiometric limit. This excess Cu leads to a decrease in vacancies and thus hole density and an increase in charge carrier scattering. This phenomenon is further observed in the doped alloys also which exhibit a lower electrical conductivity compared to the undoped alloy. The low-temperature coefficient of resistivity of all the alloys is an indicator of heavily doped degenerate semiconductor behavior. The single-doped alloy, $\text{Cu}_{1.9}\text{Li}_{0.1}\text{Te}$, has a slightly lower conductivity at all temperatures compared to double-doped alloy, $\text{Cu}_{1.9}\text{Li}_{0.1}\text{Te}_{0.97}\text{Se}_{0.03}$, possibly due to a small variation in vacancy and hence charge carrier

Table 1 The chemical composition, at. %, of the different alloys undoped, single doped and double doped obtained by energy dispersive X-ray analysis in the Scanning Electron Microscope is given

Nominal Composition of alloys	Cu (at. %)	Li (at. %)	Te (at. %)	Se (at. %)
Cu_2Te	70.49	0	29.51	0
$\text{Cu}_{1.9}\text{Li}_{0.1}\text{Te}$	70.72	0.82	29.28	0
$\text{Cu}_{1.9}\text{Li}_{0.1}\text{Te}_{0.97}\text{Se}_{0.03}$	69.10	1.05	28.97	1.92

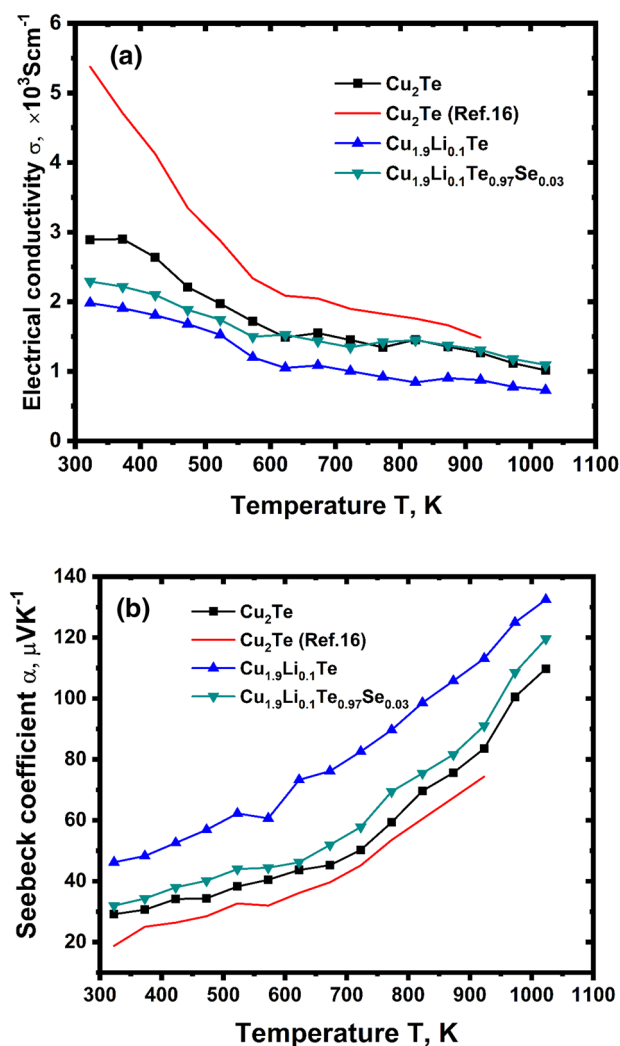


Fig. 2 **a** Electrical conductivity σ of all the alloys has a degenerate semiconductor temperature dependence. The undoped alloy has a higher electrical conductivity at all temperatures, while the pure Cu_2Te alloy reported in literature Ref. [16] has the highest values. The low-temperature dependence observed in the present work is due to an extrinsic behavior. **b** The Seebeck coefficient α increases with increasing temperature for all the alloys. The single-doped alloy has the highest α compared to the double-doped alloy while the undoped alloy has the lowest α

concentration. The substitution of Te with isoelectronic Se does not change effective carrier concentration and so has no effect on electrical conductivity. The Seebeck coefficient of all the alloys is positive in the complete temperature range due to hole dominant charge transport. It increases with increasing temperature, Fig. 2b, and the absolute value of Seebeck coefficient of undoped and doped alloys is higher than reported values (Ref. [16]). The Seebeck coefficient of single-doped alloy, $\text{Cu}_{1.9}\text{Li}_{0.1}\text{Te}$, is the highest, in agreement with electrical conductivity results. The temperature dependence does not exhibit a peak or saturation behavior

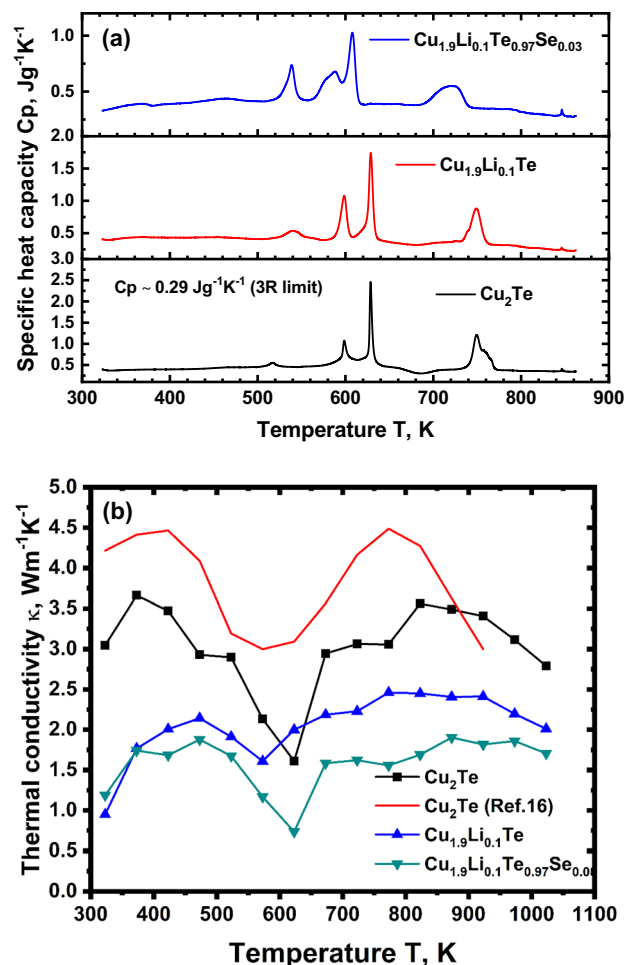


Fig. 3 **a** The specific heat capacity C_p of the undoped alloy exhibits 5 distinct transitions at 520 K, 600 K, 635 K, 750 K and 850 K. These represent equilibrium polymorphic transitions which are also observed in both single-doped and double-doped alloys but at slightly different temperatures. **b** The total thermal conductivity κ determined by measuring specific heat capacity, thermal diffusivity and density is shown here. The double-doped alloy has the lowest κ varying between $1 \text{ Wm}^{-1} \text{K}^{-1}$ to $1.75 \text{ Wm}^{-1} \text{K}^{-1}$

in the range 323–1023 K indicating the robustness of charge carriers and bipolar nature does not manifest for $T \leq 1023 \text{ K}$. The variation of specific heat capacity C_p of the 3 alloys is shown in Fig. 3a and shows clear structural phase transitions at 5 distinct temperatures. These transition temperatures are nearly identical in the undoped and single-doped alloys, Cu_2Te and $\text{Cu}_{1.9}\text{Li}_{0.1}\text{Te}$, respectively, while they are reduced in the dual substituted alloy. These polymorphic transitions are equilibrium in nature and have been observed earlier by a combination of techniques—calorimetry, X-ray diffraction and transmission electron microscopy [25]. The transition temperature is a function of the chemical composition including vacancies which in turn changes the carrier concentration [26]. Even in undoped alloys, the transition temperatures have been observed to vary depending on the

method of synthesis as well as the extent of non-stoichiometry. The thermal conductivity has been determined by measuring the specific heat capacity and thermal diffusivity and is shown in Fig. 3b. The thermal conductivity of undoped alloy varies very little with temperature— $3 \text{ W m}^{-1} \text{ K}^{-1}$ at 323 K to $2.75 \text{ W m}^{-1} \text{ K}^{-1}$ at 1023 K but has a clear peak between 500 and 700 K and reduces to a lowest value of $\sim 1.6 \text{ W m}^{-1} \text{ K}^{-1}$ at $\sim 630 \text{ K}$. This behavior is observed even in the single- and double-doped alloys but at slightly different temperatures. In general, thermal conductivity of doped alloys is much lower compared to the undoped alloy at all temperatures. The double-doped alloy has the lowest thermal conductivity with the lowest peak value reaching $\sim 0.75 \text{ W m}^{-1} \text{ K}^{-1}$ at 630 K. These results clearly show that double doping affects phonon scattering much more compared to charge carrier scattering. The absence of a clear peak-like behavior in charge transport phenomena, electrical conductivity and Seebeck coefficient, shows that polymorphic structural transitions do not change the electronic band structure significantly. The variation of these properties is rather monotonous with temperature.

The variation of power factor, Fig. 4a and figure-of-merit zT , Fig. 4b of all the different alloys together with literature values of undoped alloy are shown with respect to temperature T . The power factor of single-doped alloy for $T < 800 \text{ K}$ is highest among all the alloys due to its high Seebeck coefficient. For $T > 800 \text{ K}$, the double-doped alloy is highly promising. The figure-of-merit which considers thermal conductivity together with the power factor shows clearly that double-doped alloy has the best performance parameters at high temperature due to its low thermal conductivity. The power factor of this alloy is $\sim 16 \mu\text{W cm}^{-1} \text{ K}^{-2}$, $\sim 33\%$ higher compared to the undoped alloy, $12 \mu\text{W cm}^{-1} \text{ K}^{-2}$, synthesized in the present work. The zT of this undoped alloy is enhanced by $\sim 50\%$ by single-element doping, i.e., Li, which increases further to ~ 1.0 at 1023 K due to double doping with Li and Se for Cu and Te, respectively. These results clearly show the potential of these alloys for thermoelectric energy conversion. To check the stability and reproducibility of the dual-doped alloys, electrical conductivity and Seebeck coefficient were measured after few months. It was found that the data were reproducible within experimental variations and there was no significant hysteresis between heating and cooling.

The charge transport and hence the electronic band structure are strong functions of chemical composition of Cu_2Te [17]. The stoichiometric alloy has been reported to be unstable to decompose to Cu_{2-3}Te and Cu leading to the formation of Cu vacancies. Formation of these vacancies changes the alloy from being semiconducting with a band gap of 0.26 eV to becoming a heavily doped system with hole dominant charge transport. The vacancy defects have been predicted to push the Fermi level deep into the valence band resulting in the formation of a doped semiconductor with holes as

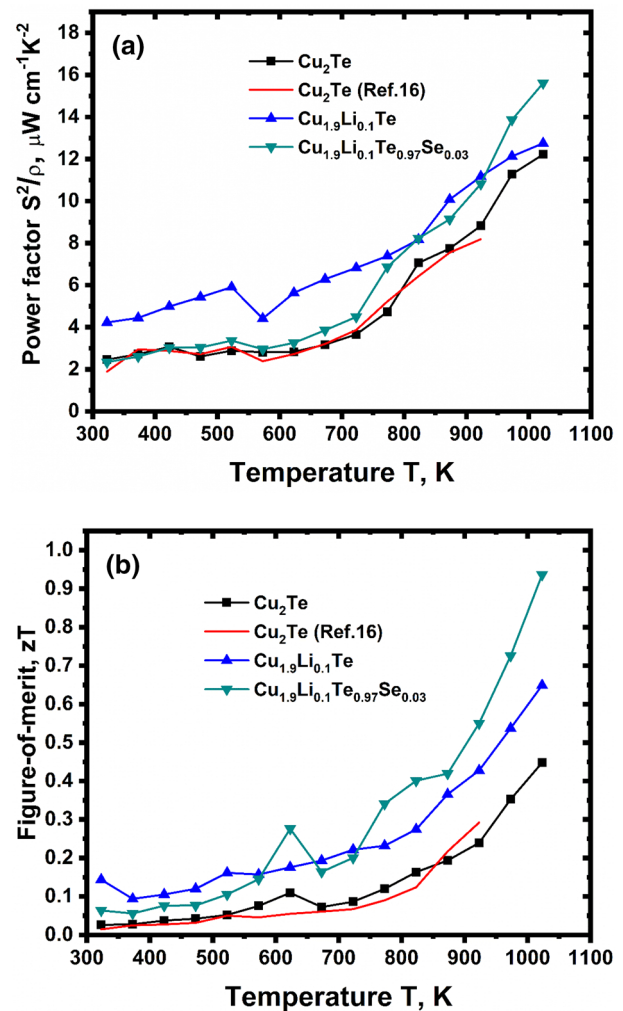


Fig. 4 **a** Power factor of single-doped alloy with the nominal composition $\text{Cu}_{1.9}\text{Li}_{0.1}\text{Te}$ has the highest power factor for $T < 800 \text{ K}$ compared to other alloys, while the double-doped alloy is good for $T > 900 \text{ K}$. The figure-of-merit zT shown in **b** however is highest for $T > 700 \text{ K}$ for the double-doped alloy due to its low thermal conductivity

charge carriers and exhibiting a metallic behavior. Hence, substituting Cu in this alloy with elements such as Ag and Sn stabilizes Fe and thus leads to reduced vacancies and carrier concentration. The reduced carrier concentration leads to lowered electrical conductivity, a relatively higher Seebeck coefficient and hence a higher zT . In the present work however, there is no clear indication for the presence of Cu in any of the 3 alloys—undoped, single doped and double doped either in the X-ray diffraction patterns or the microstructure as observed in scanning of electron microscopy. The chemical composition of the alloys determined using a combination of ICP-AES and EDS clearly shows an excess of Cu over the stoichiometric value. The results clearly show that the alloys do not have Cu vacancies but instead excess Cu in the crystal. The additional Cu together with Li results

in charge carrier scattering, while substitution of isoelectronic Se results in phonon scattering. A combination of these phenomena leads to decreased electrical and thermal conductivities, an increased Seebeck coefficient and hence an enhanced figure-of-merit zT .

4 Conclusions

The thermoelectric properties of Cu_2Te have been enhanced by double doping at both the sites, i.e., Cu and Te. The doping at Cu sites is with a monovalent alkali metal Li, while that at Te sites is with an isoelectronic chalcogen Se. At high temperatures, the double-doped alloy however exhibits a superior performance due to its lower thermal conductivity. These substitutions have been found to be highly effective in reducing the total charge carrier concentration as well as increase their mass, which results in reducing electrical conductivity and increasing the Seebeck coefficient compared to the undoped alloy. The formation of an over-stoichiometric Cu_2Te with excess Cu results in reducing the Cu vacancies and thus the charge carrier concentration significantly. The thermal conductivity reduction is due to alloy scattering phenomenon introduced by Li and Se. Addition of Li also changes the nature of its bonding with Te to ionic, compared to the predominantly covalent bonding between Cu and Te. In order for this alloy to become viable for practical applications, the medium temperature figure-of-merit also needs to be increased so that it can exhibit a high zT over the whole temperature range.

Acknowledgements The authors wish to acknowledge DST and ISRO, Government of India and Central Facilities, Indian Institute of Technology Bombay for the support.

References

1. M. Hong, Z.G. Chen, J. Zou, *Chin. Phys. B* **27**, 048403 (2018)
2. J.P. Heremans, V. Jovovic, E.S. Toberer, A. Saramat, K. Kurosaki, A. Charoenphakdee, S. Yamanaka, G.J. Snyder, *Science* **321**, 554–557 (2008)
3. Y. Pei, A. LaLonde, S. Iwanaga, G.J. Snyder, *Energy Environ. Sci.* **4**, 2085 (2011)
4. Y. Pei, A.D. LaLonde, N.A. Heinz, G.J. Snyder, *Adv. Energy Mater.* **2**, 670–675 (2012)
5. H. Beyer, J. Nurnus, H. Böttner, A. Lambrecht, E. Wagner, G. Bauer, *Phys. E* **13**, 965–968 (2002). [https://doi.org/10.1016/S1386-9477\(02\)00246-1](https://doi.org/10.1016/S1386-9477(02)00246-1)
6. F. El Akkad, B. Mansour, T. Hendeya, *Mater. Res. Bull.* **16**, 535–539 (1981). [https://doi.org/10.1016/0025-5408\(81\)90119-7](https://doi.org/10.1016/0025-5408(81)90119-7)
7. C. Zhou, Y. Yu, Y.K. Lee, O. Cojocaru-Mirédin, B. Yoo, S.P. Cho, J. Im, M. Wuttig, T. Hyeon, I. Chung, *J. Am. Chem. Soc.* **140**, 15535–15545 (2018). <https://doi.org/10.1021/jacs.8b10448>
8. L. Yang, Z.G. Chen, G. Han, M. Hong, L. Huang, J. Zou, *J. Mater. Chem. A* **4**, 9213–9219 (2016). <https://doi.org/10.1039/c6ta02998a>
9. R. Nunna, P. Qiu, M. Yin, H. Chen, R. Hanus, Q. Song, T. Zhang, M.Y. Chou, M.T. Agne, J. He, G.J. Snyder, X. Shi, L. Chen, *Energy Environ. Sci.* **10**, 1928–1935 (2017). <https://doi.org/10.1039/c7ee01737e>
10. K. Okamoto, *Jpn. J. Appl. Phys. Part 1 Regul. Pap. Short Notes Rev. Pap.* **10**, 508 (1971). <https://doi.org/10.1143/JJAP.10.508>
11. H. Liu, X. Shi, F. Xu, L. Zhang, W. Zhang, L. Chen, Q. Li, C. Uher, T. Day, G. Snyder Jeffrey, *Nat. Mater.* **11**, 422–425 (2012)
12. A. Bohra, R. Bhatt, S. Bhattacharya, R. Basu, S. Ahmad, A. Singh, D.K. Aswal, S.K. Gupta, *AIP Conf. Proc.* **1731**, 110010 (2016)
13. M.M. Mallick, S. Vitta, *J. Appl. Phys.* **122**, 024903 (2017). <https://doi.org/10.1063/1.4993900>
14. K. Sridhar, K. Chattopadhyay, *J. Alloys Compd.* **264**, 293–298 (1998)
15. Y. He, T. Zhang, X. Shi, S.H. Wei, L. Chen, *NPG Asia Mater.* **7**, e210 (2015). <https://doi.org/10.1038/am.2015.91>
16. S. Ballikaya, H. Chi, J.R. Salvador, C. Uher, *J. Mater. Chem. A* **1**, 12478 (2013)
17. Y. Qiu, Y. Liu, J. Ye, J. Li, L. Lian, *J. Mater. Chem. A* **6**, 18928–18937 (2018). <https://doi.org/10.1039/c8ta04993a>
18. S. Sarkar, P.K. Sarswat, S. Saini, P. Mele, M.L. Free, *Sci. Rep.* **9**, 8180 (2019). <https://doi.org/10.1038/s41598-019-43911-2>
19. K. Zhao, K. Liu, Z. Yue, Y. Wang, Q. Song, J. Li, M. Guan, Q. Xu, P. Qiu, H. Zhu, L. Chen, X. Shi, *Adv. Mater.* **31**, 1903480 (2019). <https://doi.org/10.1002/adma.201903480>
20. M. Li, Y. Luo, G. Cai, X. Li, X. Li, Z. Han, X. Lin, D. Sarker, J. Cui, *J. Mater. Chem. A* **7**, 2360–2367 (2019). <https://doi.org/10.1039/c8ta10741f>
21. N. Vouroutzis, C. Manolikas, *Phys. Status Solidi* **111**, 491–497 (1989). <https://doi.org/10.1002/pssa.2211110213>
22. A.A. Sirusi, A. Page, C. Uher, J.H. Ross, *J. Phys. Chem. Solids* **106**, 52–57 (2017). <https://doi.org/10.1016/j.jpcs.2017.02.016>
23. L. Yu, K. Luo, S. Chen, C.-G. Duan, *CrystEngComm* **17**, 2878–2885 (2015)
24. Y. Zhang, B. Sa, J. Zhou, Z. Sun, *Comput. Mater. Sci.* **81**, 163–169 (2014)
25. A.S. Pashinkin, V.A. Fedorov, *Inorg. Mater.* **39**, 539–554 (2003)
26. Y.G. Asadov, L.V. Rustamova, G.B. Gasimov, K.M. Jafarov, A.G. Babajev, *Phase Transitions* **38**, 247–259 (1992)

Publisher's Note Springer Nature remains neutral with regard to jurisdictional claims in published maps and institutional affiliations.